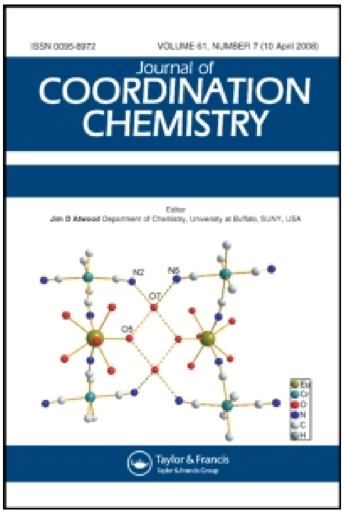

Journal of Coordination Chemistry
Publication details, including instructions for authors and subscription information:
http://www.informaworld.com/smpp/title~content=t713455674

NICKEL(II) COMPLEXES OF TRIDENTATE *N,N,O*-DONOR LIGANDS: SYNTHESES, STRUCTURES AND REDOX PROPERTIES

Galla Venkata Karunakar[a]; Nimma Rajaiah Sangeetha[a]; Vishnubhatla Susila[a]; Samudranil Pal[a]
[a] School of Chemistry, University of Hyderabad, Hyderabad, India

To cite this Article Karunakar, Galla Venkata , Sangeetha, Nimma Rajaiah , Susila, Vishnubhatla and Pal, Samudranil(2000) 'NICKEL(II) COMPLEXES OF TRIDENTATE *N,N,O*-DONOR LIGANDS: SYNTHESES, STRUCTURES AND REDOX PROPERTIES', Journal of Coordination Chemistry, 50: 1, 51 — 63

To link to this Article: DOI: 10.1080/00958970008054924

URL: http://dx.doi.org/10.1080/00958970008054924

J. Coord. Chem., 2000, Vol. 50, pp. 51–63
Reprints available directly from the publisher
Photocopying permitted by license only

Published by license under
the Gordon and Breach Science
Publishers imprint.
Printed in Malaysia.

NICKEL(II) COMPLEXES OF TRIDENTATE *N,N,O*-DONOR LIGANDS: SYNTHESES, STRUCTURES AND REDOX PROPERTIES

GALLA VENKATA KARUNAKAR,
NIMMA RAJAIAH SANGEETHA, VISHNUBHATLA SUSILA
and SAMUDRANIL PAL*

School of Chemistry, University of Hyderabad, Hyderabad 500 046, India

(Received 26 May 1999)

Nickel(II) complexes ([NiL$_2$]) of tridentate Schiff bases (HL) containing amide functionality are described. The Schiff bases, Hpabh and Hpamh (H refers to the dissociable amide proton), are derived from 2-pyridinecarboxaldehyde and benzhydrazide, and 2-pyridinecarboxaldehyde and 4-methoxybenzhydrazide, respectively. The reaction of two equivalents of HL and one equivalent of Ni(O$_2$CCH$_3$)$_2\cdot$4H$_2$O in methanol affords [NiL$_2$] in high yield. The complexes are characterised by analytical, spectroscopic, magnetic and electrochemical techniques. The structures of both complexes have been determined by X-ray crystallography. The distorted octahedral NiN$_4$O$_2$ sphere in each complex is assembled by the two meridional *N,N,O*-donor ligands. Each ligand binds the metal ion *via* the pyridine-*N*, imine-*N* and deprotonated amide-*O* atoms. The solid state room temperature (298 K) magnetic moments are consistent with a d^8 ($S = 1$) ground state electronic configuration. Electronic spectra of the complexes in CH$_3$CN solutions display the ν_1 band at ~850 nm followed by charge transfer bands in the range 381–241 nm. The [Ni^{III}L$_2$]$^+$–[Ni^{II}L$_2$] couple was observed in the cyclic voltammograms of both complexes. The potentials are 0.97 and 0.91 V (*versus* Ag–AgCl) for [Ni(pabh)$_2$] and [Ni(pamh)$_2$], respectively.

Keywords: Nickel(II) complex; X-ray structure; amide-*O* coordination; redox

INTRODUCTION

In recent years the chemistry of higher-valent (> +2) nickel has received considerable attention due to it's participation in the functions of various metalloenzymes.[1,2] Ligands containing the deprotonated amide function

---

* Corresponding author.

which coordinates through the nitrogen atom are well known to stabilise higher-valent late first transition series metal ions.[3] This type of complex can be unstable due to electron transfer from the ligand to the metal ion involving the hydrogen at the carbon atom α to the coordinated nitrogen.[4–7] One option to prevent such a proton coupled redox process is replacement of the α-hydrogen with an alkyl or aryl group.[8] Another option is coordination of the deprotonated amide oxygen instead of the nitrogen. However amide oxygen coordinated higher-valent species are rare.[9–11] The objective of this study is to examine whether aroylhydrazones of 2-pyridinecarboxaldehyde (HL, where H refers to the dissociable amide proton which can coordinate a metal ion *via* pyridine-*N*, imine-*N* and amide-*O* atoms) are able to produce nickel(III) species. In this work we report the synthesis, structure and properties of two complexes having nickel(II) in an N_4O_2 coordination sphere assembled by two monobasic, tridentate, meridionally spanning ligands. The complexes are characterised by analytical, spectroscopic, magnetic and X-ray crystallographic studies. The complexes are indeed redox active and display near reversible nickel(II) to nickel(III) oxidation.

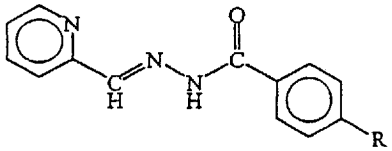

Hpabh (R = H)
Hpamh (R = OMe)

EXPERIMENTAL

Materials

The chemicals and solvents used in this work were of analytical grade available commercially and were used without further purification.

Physical Measurements

Microanalytical (C, H, N) data were obtained with a Perkin-Elmer Model 240C elemental analyser. Electronic spectra were recorded on a Jasco-7800 spectrophotometer. Infrared spectra were collected by using KBr pellets on a Jasco-5300 FT-IR spectrophotometer. Room temperature solid state magnetic susceptibilities were measured by using a Cahn magnetic susceptibility system consisting of a model 4600 adjustable gap electromagnet and a model 1000 electrobalance. Diamagnetic corrections calculated from Pascal's constants[12] were used to obtain the molar paramagnetic susceptibilities. Solution electrical conductivities were measured with a Digisun DI-909 conductivity meter. A Cypress model CS-1090/CS-1087 electroanalytical system was used for cyclic voltammetric experiments with acetonitrile solutions of the complexes containing tetrabutylammonium perchlorate (TBAP) as supporting electrolyte. The three electrode measurements were carried out at 298 K under a dinitrogen atmosphere with a platinum disk working electrode, a platinum wire auxiliary electrode and an Ag–AgCl reference electrode. Coulometric experiments were performed using a PAR 179 digital coulometer, a 377A cell system, and a platinum-wire-gauze working electrode. The potentials reported in this work are uncorrected for junction contributions.

Preparation of Compounds

The Schiff bases, Hpabh and Hpamh, were prepared in high yield (75–90%) from methanol by condensation of one equivalent of 2-pyridinecarboxaldehyde with one equivalent of benzhydrazide and 4-methoxybenzhydrazide, respectively.

[Ni(pabh)$_2$]

To a methanol solution (15 cm^3) of Hpabh (180 mg, 0.8 mmol) was added 100 mg (0.4 mmol) of $Ni(O_2CCH_3)_2 \cdot 4H_2O$ and the mixture was refluxed for 4 h. It was then cooled to room temperature and a brown crystalline solid separated. The solid was collected by filtration, washed with ice-cold methanol and dried under vacuum. Yield: (110 mg; 54%). Elemental analysis data are as follows. Found: C, 61.42; H, 3.89; N, 16.46%. Calcd. for $NiC_{26}H_{20}N_6O_2$: C, 61.57; H, 3.97; N, 16.57%. Selected IR bands (cm^{-1}) (Symbols: s, strong; m, medium; w, weak): 1601(s), 1555(m), 1487(s), 1462(s), 1339(s), 1289(s), 1142(m), 1078(s), 920(w), 712(m), 691(m), 523(w).

[Ni(pamh)$_2$] was prepared by following the same procedure as described above from Hpamh and $Ni(O_2CCH_3)_2 \cdot 4H_2O$ in 60% yield. Elemental analysis data are as follows. Found: C, 59.03; H, 4.14; N, 14.53%. Calcd. for $NiC_{28}H_{24}N_6O_4$: C, 59.29; H, 4.26; N, 14.82%. Selected IR bands (cm^{-1}) (Symbols: s, strong; m, medium; w, weak): 1603(s), 1514(m), 1487(s), 1456(s), 1352(s), 1250(s), 1167(s), 1078(s), 1026(m), 922(w), 843(w), 766(m), 677(m), 615(w).

X-Ray Structure Determination

Single crystals of both complexes were grown by slow evaporation of acetonitrile–toluene (1 : 1) solutions. In each case the crystal was mounted at the end of a glass fibre and the data were collected on an Enraf-Nonius Mach-3 single crystal diffractometer using graphite-monochromated MoKα radiation ($\lambda = 0.71073$ Å) by the ω-scan method. Unit cell parameters of [Ni(pabh)$_2$] and [Ni(pamh)$_2$] were determined by least-squares fit of 25 reflections having 2θ values in the range 20–24° and 18–21°, respectively. Stability of the crystal was monitored by measuring the intensities of three check reflections after every 1.5 h during the data collection. No decay was observed in the 48 h ([Ni(pabh)$_2$]) and 42 h ([Ni(pamh)$_2$]) of exposure to X-ray. The data were corrected for Lorentz-polarisation effects. No absorption correction was applied. The structures were solved by direct methods and refined by full-matrix least-squares on F^2 and Fourier techniques. [Ni(pabh)$_2$] and [Ni(pamh)$_2$] crystallise in $P2_1/n$ and $P\bar{1}$ space groups, respectively. In each case the asymmetric unit contains a single molecule of the complex. For both structures all the non-hydrogen atoms were refined anisotropically. Hydrogen atoms were added at calculated positions by using a riding model for structure factor calculations, but were not refined. Calculations were performed using the programs of the Xtal software[13] package for data reduction, and SHELX-97 programs[14] for structure solution and refinement. The ORTEX6a package[15] was used for molecular graphics. Significant crystal data are summarised in Table I. The final atomic coordinates and equivalent isotropic thermal parameters for [Ni(pabh)$_2$] and [Ni(pamh)$_2$] are listed in Tables II and III, respectively.

RESULTS AND DISCUSSION

Synthesis and Properties

The dark brown nickel(II) complexes were synthesised in good yields by reacting one equivalent of $Ni(O_2CCH_3)_2 \cdot 4H_2O$ with two equivalents of the ligands in boiling methanol. Elemental analyses are satisfactory with empirical formula, [NiL$_2$] ($L^- =$ pabh$^-$, pamh$^-$). Room temperature (298 K) solid state magnetic moments obtained are 3.12 and 2.99 μ_B for [Ni(pabh)$_2$] and

TABLE I Crystallographic data for [Ni(pabh)$_2$] and [Ni(pamh)$_2$]

Compound	[Ni(pabh)$_2$]	[Ni(pamh)$_2$]
Crystal size (mm)	0.26 × 0.18 × 0.43	0.20 × 0.32 × 0.36
Chemical formula	$NiC_{26}H_{20}N_6O_2$	$NiC_{28}H_{24}N_6O_4$
Crystal system	Monoclinic	Triclinic
Space group	$P2_1/n$	$P\bar{1}$
a/Å	9.6724(12)	10.5796(14)
b/Å	23.835(3)	11.2431(14)
c/Å	10.2763(10)	12.8080(19)
α/°	90	114.819(12)
β/°	105.25(2)	111.401(12)
γ/°	90	90.421(11)
Volume/Å^3	2285.7(4)	1264.0(3)
Z	4	2
D(calcd.)/g cm^{-3}	1.474	1.490
μ/cm^{-1}	8.86	8.16
Reflections collected	4373	4445
No. of unique reflections	4012	4445
No. of observed reflections	2642 [$I > 2\sigma(I)$]	2778 [$I > 2\sigma(I)$]
$R1$[a]	0.0358	0.0395
$wR2$[b]	0.1083	0.0783
Goodness-of-fit[c]	1.155	1.086
Largest diff. peak and hole (e/Å^3)	0.449 and −0.461	0.316 and −0.356

[a] $R1 = \sum||F_o| - |F_c||/\sum|F_o|$. [b] $wR2 = \{\sum[(F_o^2 - F_c^2)^2]/\sum[w(F_o^2)^2]\}^{1/2}$. [c] Goodness-of-fit $= \{\sum[w(F_o^2 - F_c^2)^2]/(N_{\text{observns}} - N_{\text{parameters}})\}^{1/2}$; $w = 1/[\sigma^2(F_o^2) + (aP)^2 + bP]$ ($a = 0.0669$ and 0.0397 for [Ni(pabh)$_2$] and [Ni(pamh)$_2$] respectively; $b = 0.0$ for both), where $P = [2F_c^2 + \max(F_o^2, 0)]/3$.

[Ni(pamh)$_2$], respectively. These values are conforming with an $S = 1$ spin state in each complex. The complexes are electrically non-conducting in solutions.

Infrared spectra of the complexes do not display the peaks corresponding to the amide functionality[16,17] of the free ligands. A strong band observed at ~1602 cm^{-1} is most probably due to the conjugate C=N–N=C moiety.[18] Thus in each complex the ligands are in the enolate form and act as a monobasic tridentate *N,N,O* donors.

In acetonitrile solutions the electronic spectra of the complexes are very similar. Each complex displays (Table IV) a weak absorption at ~850 nm followed by three intense bands in the range 381–241 nm (Figure 1). The lowest energy band corresponds to the ν_1 transition for an octahedral nickel(II) complex. The following intense absorptions are most likely due to charge-transfer and intraligand transitions. In general the band positions for [Ni(pamh)$_2$] are at lower energy compared to those for [Ni(pabh)$_2$]. Such a red shift has been observed before for some manganese, iron and copper complexes when the substituent on the coordinated ligand becomes more electron releasing.[7,9,19–22]

TABLE II Atomic coordinates ($\times 10^4$) and equivalent isotropic thermal parameters[a] ($Å^2 \times 10^3$) for [Ni(pabh)$_2$]

Atom	*x/a*	*y/b*	*z/c*	*U(eq)*
Ni	3438(1)	1007(1)	6330(1)	35(1)
O(1)	1978(3)	1405(1)	4717(3)	42(1)
O(2)	5321(3)	1350(1)	5927(3)	44(1)
N(1)	4689(3)	313(1)	7276(3)	40(1)
N(2)	2669(3)	384(1)	5062(3)	36(1)
N(3)	1501(3)	484(1)	4004(3)	39(1)
N(4)	1830(3)	964(1)	7400(3)	36(1)
N(5)	4091(3)	1587(1)	7742(3)	36(1)
N(6)	5342(3)	1869(1)	7837(3)	39(1)
C(1)	5764(5)	298(2)	8388(4)	54(1)
C(2)	6574(5)	−178(2)	8807(4)	61(1)
C(3)	6271(5)	−653(2)	8044(4)	57(1)
C(4)	5159(4)	−646(2)	6881(4)	47(1)
C(5)	4388(4)	−157(2)	6524(4)	38(1)
C(6)	3200(4)	−106(2)	5320(4)	40(1)
C(7)	1240(4)	1034(2)	3962(4)	37(1)
C(8)	−80(4)	1214(2)	2915(4)	36(1)
C(9)	−1209(4)	848(2)	2457(4)	49(1)
C(10)	−2440(5)	1017(2)	1526(4)	56(1)
C(11)	−2543(5)	1553(2)	1027(4)	56(1)
C(12)	−1445(5)	1921(2)	1481(4)	61(1)
C(13)	−209(5)	1756(2)	2439(4)	51(1)
C(14)	650(4)	649(2)	7188(4)	45(1)
C(15)	−279(4)	669(2)	7987(4)	54(1)
C(16)	−25(5)	1043(2)	9046(5)	54(1)
C(17)	1172(4)	1384(2)	9264(4)	47(1)
C(18)	2081(4)	1335(2)	8434(4)	37(1)
C(19)	3364(4)	1670(2)	8599(4)	40(1)
C(20)	5884(4)	1704(2)	6823(4)	37(1)
C(21)	7280(4)	1971(2)	6835(4)	39(1)
C(22)	7921(4)	2352(2)	7830(4)	48(1)
C(24)	9912(5)	2447(2)	6897(6)	67(1)
C(23)	9232(5)	2596(2)	7868(5)	59(1)
C(25)	9304(5)	2072(2)	5900(5)	63(1)
C(26)	7972(5)	1837(2)	5849(5)	51(1)

[a] *U(eq)* is defined as one third of the trace of the orthogonalized U_{ij} tensor.

Description of Structures

The molecular structures of [Ni(pabh)$_2$] and [Ni(pamh)$_2$] are depicted in Figures 2 and 3, respectively. Selected bond distances and angles are listed in Tables V and VI. The bond distances and angles clearly indicate a large distortion of the NiN_4O_2 octahedra. In each complex the nickel(II) ion is coordinated to the pyridine-*N*, the imine-*N* and the deprotonated amide-*O* atoms of the planar tridentate ligands. Two five membered chelate rings are formed by each ligand. The average chelate bite angle formed by the pyridine-*N* and imine-*N* is slightly larger than that formed by the amide-*O*

TABLE III Atomic coordinates ($\times 10^4$) and equivalent isotropic thermal parameters[a] ($Å^2 \times 10^3$) for $[Ni(pamh)_2]$

Atom	*x/a*	*y/b*	*z/c*	*U(eq)*
Ni	4322(1)	1290(1)	7400(1)	35(1)
O(1)	3700(2)	3063(2)	7396(2)	42(1)
O(2)	1315(3)	7254(2)	5440(3)	55(1)
O(3)	6398(2)	2000(2)	7909(2)	40(1)
O(4)	12878(3)	4068(3)	11022(3)	72(1)
N(1)	4583(3)	−713(3)	6549(2)	36(1)
N(2)	3386(3)	803(3)	5588(2)	32(1)
N(3)	2813(3)	1731(3)	5232(2)	34(1)
N(4)	2634(3)	760(3)	7722(2)	36(1)
N(5)	5251(3)	1637(3)	9186(2)	34(1)
N(6)	6643(3)	2073(3)	9816(2)	38(1)
C(1)	5203(4)	−1471(4)	7067(4)	45(1)
C(2)	5304(4)	−2768(4)	6386(4)	51(1)
C(3)	4758(4)	−3298(4)	5102(4)	48(1)
C(4)	4120(3)	−2543(3)	4527(3)	38(1)
C(5)	4031(3)	−1252(3)	5276(3)	33(1)
C(6)	3369(3)	−363(3)	4771(3)	34(1)
C(7)	3063(3)	2877(3)	6267(3)	32(1)
C(8)	2591(3)	4021(3)	6032(3)	34(1)
C(9)	1931(4)	3866(3)	4817(3)	40(1)
C(10)	1485(4)	4911(3)	4578(3)	40(1)
C(11)	1692(4)	6153(4)	5572(3)	40(1)
C(12)	2335(4)	6325(4)	6796(3)	43(1)
C(13)	2763(3)	5275(3)	7021(3)	40(1)
C(14)	638(4)	7104(4)	4196(4)	58(1)
C(15)	1310(4)	296(4)	6953(3)	44(1)
C(16)	327(4)	−109(4)	7257(4)	51(1)
C(17)	747(4)	−26(4)	8442(4)	56(1)
C(18)	2112(4)	446(4)	9257(4)	55(1)
C(19)	3037(4)	847(4)	8894(3)	38(1)
C(20)	4511(4)	1355(4)	9681(3)	41(1)
C(21)	7129(3)	2223(3)	9036(3)	35(1)
C(22)	8649(3)	2699(3)	9552(3)	37(1)
C(23)	9532(4)	2862(4)	10736(3)	53(1)
C(24)	10929(4)	3305(4)	11178(4)	60(1)
C(25)	11479(4)	3623(4)	10478(4)	50(1)
C(26)	10609(4)	3472(4)	9307(4)	48(1)
C(27)	9207(4)	3010(4)	8864(3)	43(1)
C(28)	13468(4)	4497(4)	10373(4)	70(1)

[a] *U(eq)* is defined as one third of the trace of the orthogonalized U_{ij} tensor.

and imine-*N*. The former is 77.83° and 78.43° and the latter is 75.91° and 76.28° for $[Ni(pabh)_2]$ and $[Ni(pamh)_2]$, respectively. The average N–N, N–C and C–O distances in the =N–N=C(O$^-$)– moiety of the ligands in both complexes are consistent with the enolate form of the amide functions.[11,22–30] They are 1.366, 1.337 and 1.263 Å and 1.364, 1.341 and 1.273 Å for $[Ni(pabh)_2]$ and $[Ni(pamh)_2]$, respectively. The Ni–*N*(pryridine), Ni–*N*(imine) and Ni–*O* bond distances observed in these two complexes are

TABLE IV ·Electronic spectroscopic and cyclic voltammetric[a] data in acetonitrile at 298 K

Complex	λ_{max}/nm (ε/M^{-1} cm^{-1})	$E_{1/2}{}^{b}$/V	$\Delta E_p{}^{c}$/mV
[Ni(pabh)$_2$]	851(41), 375(27800), 291(19550), 241(23270)	0.97	60
[Ni(pamh)$_2$]	853(32), 381(28000), 304(21800), 243(19800)	0.91	80

[a] Supporting electrolyte is tetrabutylammonium perchlorate (0.1 M); working electrode is platinum; reference electrode is Ag–AgCl. [b] $E_{1/2}$ is calculated as the average of anodic (E_{pa}) and cathodic (E_{pc}) peak potentials. [c] Peak to peak separation $\Delta E_p = E_{pa} - E_{pc}$.

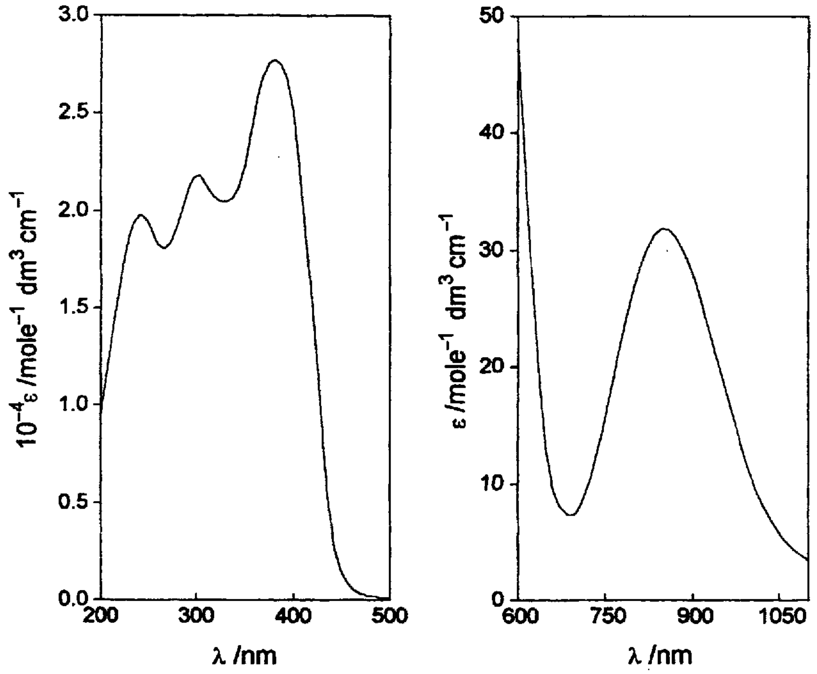

FIGURE 1 Electronic spectrum of [Ni(pamh)$_2$] in acetonitrile.

within the range reported for nickel(II) complexes having the same coordinating atoms.[24,31] There is no difference in the Ni–*N*(pyridine) distances and also in the Ni–*N*(imine) distances in [Ni(pabh)$_2$]. However the Ni–*O* distances are very different. For [Ni(pamh)$_2$] only the Ni–*N*(imine) distances are equal. In general the average Ni–*N*(imine) distances are significantly shorter than the average Ni–*N*(pyridine) distances in both complexes. Such a difference can be rationalised by considering the better π-backbonding for the Ni–*N*(imine) bond compared to that in the Ni–*N*(pyridine) bond.[24,32] For [Ni(pabh)$_2$] the average Ni–*N*(pyridine), Ni–*N*(imine) and Ni–*O* distances are 2.130, 1.984 and 2.116 Å respectively.

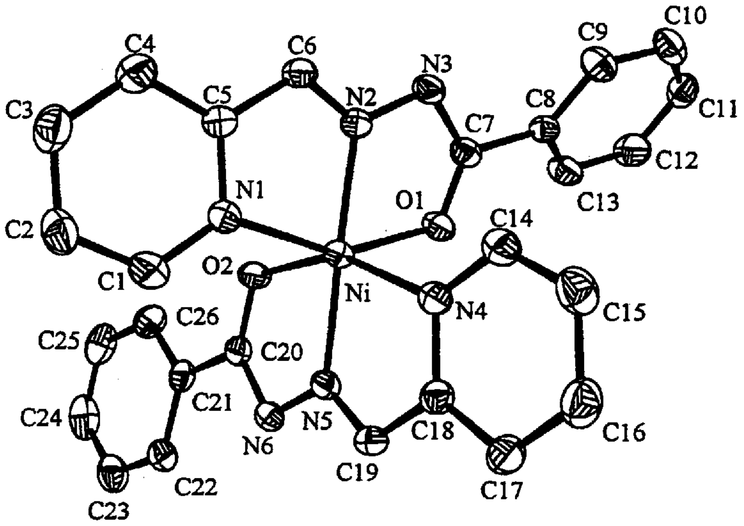

FIGURE 2 Structure and atom labelling scheme for [Ni(pabh)$_2$]. All atoms are represented by their 30% probability thermal ellipsoids. Hydrogen atoms are omitted for clarity.

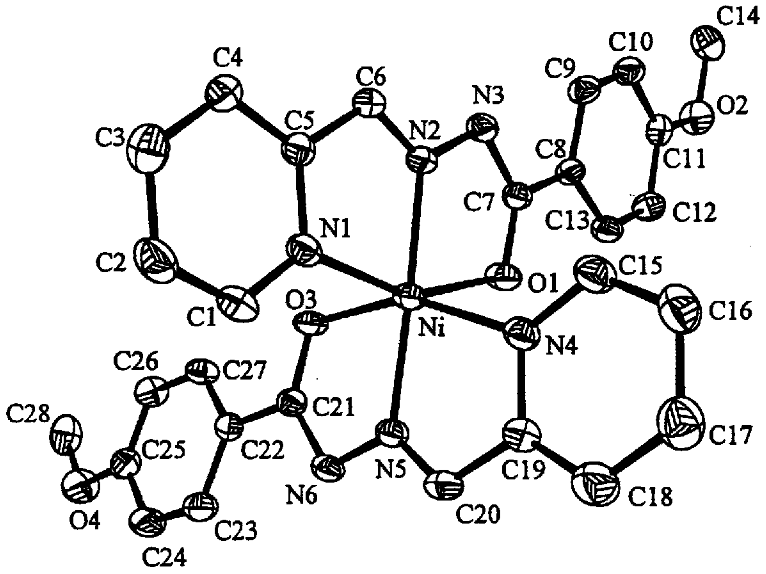

FIGURE 3 Structure of [Ni(pamh)$_2$] showing 30% probability thermal ellipsoids and the atom labelling scheme. Hydrogen atoms are omitted for clarity.

TABLE V Selected bond distances (Å) and angles (°) for $[Ni(pabh)_2]$[a]

Bond distances			
Ni–N(1)	2.129(3)	Ni–N(2)	1.988(3)
Ni–N(4)	2.131(3)	Ni–N(5)	1.983(3)
Ni–O(1)	2.099(3)	Ni–O(2)	2.133(3)
Bond angles			
N(1)–Ni–N(2)	77.71(12)	N(1)–Ni–N(4)	97.51(12)
N(1)–Ni–N(5)	100.05(12)	N(1)–Ni–O(1)	153.51(11)
N(1)–Ni–O(2)	88.55(11)	N(2)–Ni–N(4)	95.96(12)
N(2)–Ni–N(5)	173.26(12)	N(2)–Ni–O(1)	76.24(11)
N(2)–Ni–O(2)	110.53(11)	N(4)–Ni–N(5)	77.95(12)
N(4)–Ni–O(1)	89.95(11)	N(4)–Ni–O(2)	153.50(11)
N(5)–Ni–O(1)	106.37(11)	N(5)–Ni–O(2)	75.59(11)
O(1)–Ni–O(2)	96.04(10)		

[a] Numbers in parentheses are estimated standard deviations.

TABLE VI Selected bond distances (Å) and angles (°) for $[Ni(pamh)_2]$[a]

Bond distances			
Ni–N(1)	2.123(3)	Ni–N(2)	1.979(3)
Ni–N(4)	2.107(3)	Ni–N(5)	1.989(3)
Ni–O(1)	2.105(2)	Ni–O(3)	2.093(2)
Bond angles			
N(1)–Ni–N(2)	78.05(11)	N(1)–Ni–N(4)	93.35(11)
N(1)–Ni–N(5)	97.93(11)	N(1)–Ni–O(1)	154.54(10)
N(1)–Ni–O(3)	90.99(10)	N(2)–Ni–N(4)	99.99(11)
N(2)–Ni–N(5)	175.78(12)	N(2)–Ni–O(1)	76.59(10)
N(2)–Ni–O(3)	105.21(10)	N(4)–Ni–N(5)	78.82(11)
N(4)–Ni–O(1)	93.17(10)	N(4)–Ni–O(3)	154.79(10)
N(5)–Ni–O(1)	107.47(10)	N(5)–Ni–O(3)	75.98(10)
O(1)–Ni–O(3)	93.49(9)		

[a] Numbers in parentheses are estimated standard deviations.

Those for $[Ni(pamh)_2]$ are 2.115, 1.984 and 2.099 Å respectively. The reason for the difference in the average Ni–*N*(pyridine) distances in $[Ni(pamh)_2]$ and $[Ni(pabh)_2]$ is not very clear. However the smaller average Ni–*O* distance in $[Ni(pamh)_2]$ compared to that in $[Ni(pabh)_2]$ is most likely due to better Ni–*O* σ-bonding in the former compared to that in the latter. Such a difference in σ-bond strength is not unexpected as pamh$^-$ contains an electron releasing methoxy group *para* to the C–O$^-$ group. The redox potentials are also indicative to this trend.

Redox Properties

The redox behaviour of the complexes in acetonitrile solutions has been studied using cyclic voltammetry. A cyclic voltammogram of $[Ni(pabh)_2]$ is illustrated in Figure 4. Each of the two complexes displays a well defined

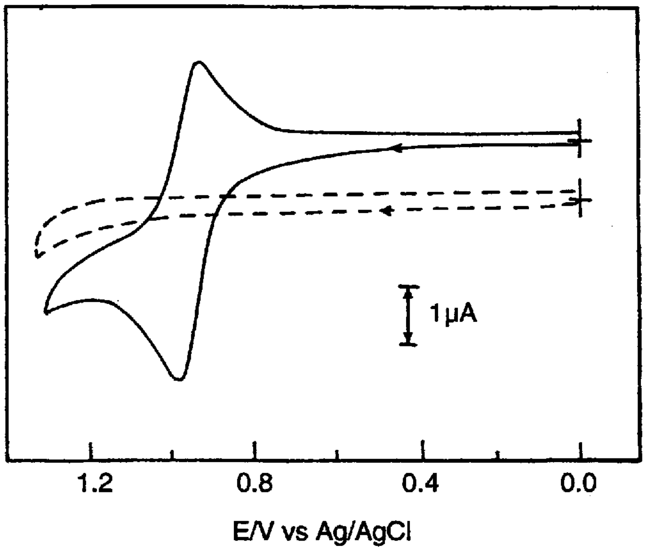

FIGURE 4 Cyclic voltammograms (scan rate 100 mV s^{-1}) of $[Ni(pabh)_2]$ (—) in acetonitrile (0.1 M TBAP) and $[Zn(pabh)_2]$ (----) in chloroform–acetonitrile (1:4; 0.1 M TBAP) at a platinum electrode at 298 K.

near reversible oxidation at potentials positive to the Ag–AgCl electrode (Table IV). The electron stoichiometry of this response could not be established by coulometry. Bulk electrolysis at potentials higher than the anodic peak potential shows a continuous coulomb count. However the one electron stoichiometry of this redox process was confirmed by comparing the current height with known one-electron redox processes under identical conditions.[33] The corresponding zinc(II) analogues (characterised by elemental analyses and infrared spectra) do not display any response up to 1.3 V (Figure 4). Thus the oxidation response observed for both complexes

$$[Ni^{III}L_2]^+ + e^- \rightleftharpoons [Ni^{II}L_2] \qquad (1)$$

is assigned to the nickel(III)–nickel(II) couple (Equation (1)). The oxidation potentials are 0.97 and 0.91 V for $[Ni(pabh)_2]$ and $[Ni(pamh)_2]$, respectively. The deprotonated amide-*O* in $pamh^-$ is expected to be a better σ-donor than that in $pabh^-$ as the former contains an electron releasing methoxy group on the aroyl moiety. The bond strength should increase with the increase in the donation ability of the coordinating atom (*vide supra*). As a result the potential will decrease with the increase in bond strength.[34] Thus the $E_{1/2}$ value observed for [Ni(pamh)$_2$] is lower than that observed for [Ni(pabh)$_2$].

In conclusion, two new nickel(II) complexes with a distorted octahedral N_4O_2 coordination sphere assembled *via* tridentate pyridine–imine–amide coordinating ligands have been reported. Amide oxygen coordinated, higher-valent species are scarcely known. There is no report of such nickel(III) species in the literature. The complexes reported in this work display a nickel(II) to nickel(III) oxidation in cyclic voltammetry and provide the first examples of such species. The observed oxidation potentials suggest that the nickel(III) species may have a possible use as moderately strong one-electron oxidising agents.

Acknowledgements

Financial assistance received from the Council of Scientific and Industrial Research, New Delhi (Grant No. 01(1422)/96/EMR-II) is gratefully acknowledged. Ms. N.R. Sangeetha thanks the University Grants Commission, New Delhi, for a research fellowship. Crystallography was performed at the National Single Crystal Diffractometer Facility, School of Chemistry, University of Hyderabad established by the Department of Science and Technology, New Delhi. Our sincere thanks are due to Professor A. Chakravorty for coulometric measurements. We are thankful to Professor P.S. Zacharias for cyclic voltammetric experiments.

Supplementary Material

Tables of intramolecular bond distances and angles, anisotropic thermal parameters, hydrogen atom positional parameters and observed and calculated structure factors for the structures reported in this work are available from the authors on request.

References

[1] J.R. Lancaster (Ed.), *The Bioinorganic Chemistry of Nickel* (VCH, New York, 1988).
[2] R. Cammack, *Adv. Inorg. Chem.*, **32**, 297 (1988).
[3] D.W. Margerum, *Pure Appl. Chem.*, **55**, 23 (1983).
[4] J.L. Kurtz, G.L. Burce and D.W. Margerum, *Inorg. Chem.*, **17**, 2454 (1978).
[5] J.S. Rybka and D.W. Margerum, *Inorg. Chem.*, **20**, 1453 (1981).
[6] T.J. Collins, K.L. Kotska, E.L. Uffelman and T.L. Weinberger, *Inorg. Chem.*, **30**, 4204 (1991).
[7] A.V. Lakshmi, N.R. Sangeetha and S. Pal, *Indian J. Chem.*, **36A**, 844 (1997).
[8] K.L. Kotska, B.G. Fox, M.P. Hendrich, T.J. Collins, C.E. Pickard, L.J. Wright and E. Münck, *J. Am. Chem. Soc.*, **115**, 6746 (1993).

[9] N.R. Sangeetha and S. Pal, *J. Coord. Chem.*, **42**, 157 (1997).
[10] S. Pal, *J. Chem. Res.* (*S*), 236 (1995).
[11] N.R. Sangeetha, C.K. Pal, P. Ghosh and S. Pal, *J. Chem. Soc., Dalton Trans.*, 3293 (1996).
[12] W.E. Hatfield, *Theory and Applications of Molecular Paramagnetism*, E.A. Boudreux and L.N. Mulay (Eds.) (Wiley, New York, 1976), p. 491.
[13] *Xtal3.4 User's Manual*, S.R. Hall, G.S.D. King and J.M. Stewart (Eds.) (University of Western Australia, Perth, 1995).
[14] G.M. Sheldrick, *SHELX-97 Structure Determination Software* (University of Göttingen, Germany, 1997).
[15] P. McArdle, *J. Appl. Crystallogr.*, **28**, 65 (1995).
[16] W. Kemp, *Organic Spectroscopy* (Macmillan, Hampshire, 1987), p. 64.
[17] K. Nakamoto, *Infrared and Raman Spectra of Inorganic and Coordination Compounds* (Wiley, New York, 1986), p. 242.
[18] L. El Sayed and M.F. Iskander, *J. Inorg. Nucl. Chem.*, **33**, 435 (1971).
[19] J.W. Pyrz, A.L. Roe, L.J. Stern and L. Que Jr., *J. Am. Chem. Soc.*, **107**, 614 (1985).
[20] R.N. Mukerjee, O.A. Rajan and A. Chakravorty, *Inorg. Chem.*, **21**, 785 (1982).
[21] R.J.P. Williams, *J. Chem. Soc.*, 137 (1955).
[22] A. Choudhury, B. Geetha, N.R. Sangeetha, V. Kavita, V. Susila and S. Pal, *J. Coord. Chem.*, **48**, 87 (1999).
[23] A. Mangia, M. Nardelli, C. Pelizzi and G. Pelizzi, *J. Chem. Soc., Dalton Trans.*, 1141 (1973).
[24] S. Seth and S. Chakraborty, *Acta Cryst.*, **C40**, 1530 (1984).
[25] S. Dutta, V. Manivannan, L.G. Babu and S. Pal, *Acta Cryst.*, **C51**, 813 (1995).
[26] M.R. Maurya, D.C. Antony, S. Gopinathan, V.G. Puranik, S.S. Tavale and C. Gopinathan, *Bull. Chem. Soc. Jpn.*, **68**, 2847 (1995).
[27] W. Wang, F.-L. Zeng, X. Wang and M.-Y. Tan, *Polyhedron*, **15**, 1699 (1996).
[28] X.-M. Zhang, X.-Z. You and X. Wang, *Polyhedron*, **15**, 1793 (1996).
[29] S.P. Rath, S. Mondal and A. Chakravorty, *Inorg. Chim Acta*, **263**, 247 (1997).
[30] N.R. Sangeetha, K. Baradi, R. Gupta, C.K. Pal, V. Manivannan and S. Pal, *Polyhedron*, **18**, 1425 (1999).
[31] M.H. Moore, L.R. Nassimbeni and M.L. Niven, *J. Chem. Soc., Dalton Trans.*, 2125 (1987).
[32] A. Seal and S. Ray, *Acta Cryst.*, **C40**, 929 (1984).
[33] S. Pal, D. Bandyopadhyay, D. Datta and A. Chakravorty, *J. Chem. Soc., Dalton Trans.*, 159 (1985).
[34] S. Dutta, P. Basu and A. Chakravorty, *Inorg. Chem.*, **30**, 4031 (1991).